Myocardial Tissue Characterization Using Magnetic Resonance Noncontrast T1 Mapping in Hypertrophic and Dilated Cardiomyopathy

Sairia Dass, MRCP, DPhil*; Joseph J. Suttie, FRACP, DPhil*; Stefan K. Piechnik, PhD; Vanessa M. Ferreira, MD; Cameron J. Holloway, MRCP, FRACP, DPhil; Rajarshi Banerjee, MRCP, MPH; Masliza Mahmod, MBChB; Lowri Cochlin, PhD; Theodoros D. Karamitsos, MD, PhD; Matthew D. Robson, PhD; Hugh Watkins, MD, PhD; Stefan Neubauer, MD

Background—Noncontrast magnetic resonance T1 mapping reflects a composite of both intra- and extracellular signal. We hypothesized that noncontrast T1 mapping can characterize the myocardium beyond that achieved by the well-established late gadolinium enhancement (LGE) technique (which detects focal fibrosis) in both hypertrophic (HCM) and dilated (DCM) cardiomyopathy, by detecting both diffuse and focal fibrosis.

Methods and Results—Subjects underwent Cardiovascular Magnetic Resonance imaging at 3T (28 HCM, 18 DCM, and 12 normals). Matching short-axis slices were acquired for cine, T1 mapping, and LGE imaging (0.1 mmol/kg). Circumferential strain was measured in the midventricular slice, and ^{31}P magnetic resonance spectroscopy was acquired for the septum of the midventricular slice. Mean T1 relaxation time was increased in HCM and DCM (HCM 1209±28 ms, DCM 1225±42 ms, normal 1178±13 ms, $P<0.05$). There was a weak correlation between mean T1 and LGE ($r=0.32$, $P<0.001$). T1 values were higher in segments with LGE than in those without (HCM with LGE 1228±41 ms versus no LGE 1192±79 ms, $P<0.01$; DCM with LGE 1254±73 ms versus no LGE 1217±52 ms, $P<0.01$). However, in both HCM and DCM, even in segments unaffected by LGE, T1 values were significantly higher than normal ($P<0.01$). T1 values correlated with disease severity, being increased as wall thickness increased in HCM; conversely, in DCM, T1 values were highest in the thinnest myocardial segments. T1 values also correlated significantly with circumferential strain ($r=0.42$, $P<0.01$). Interestingly, this correlation remained statistically significant even for the slices without LGE ($r=0.56$, $P=0.04$). Finally, there was also a statistically significant negative correlation between T1 values and phosphocreatine/adenosine triphosphate ratios ($r=-0.59$, $P<0.0001$).

Conclusions—In HCM and DCM, noncontrast T1 mapping detects underlying disease processes beyond those assessed by LGE in relatively low-risk individuals. **(*Circ Cardiovasc Imaging*. 2012;5:726-733.)**

Key Words: dilated cardiomyopathy ■ hypertrophic cardiomyopathy ■ magnetic resonance imaging ■ T1 mapping ■ tissue characterization

Cardiomyopathies encompass a diverse spectrum of inherited or acquired disorders and are an important cause of morbidity and mortality worldwide.[1–3] Hypertrophic cardiomyopatthy (HCM) affects 1 in 500 individuals and is the commonest cause of sudden cardiac death in the young (including competitive athletes).[1,2,4–6] Dilated cardiomyopatthy (DCM) is the second most common cause of heart failure after coronary artery disease and is the end phenotype of various nonischemic insults.[1,2,4,7] However, both HCM and DCM exhibit highly variable clinical outcomes. Many HCM patients remain free from clinical complications, although others carry a disproportionately high risk of sudden death[8]; some DCM patients remain stable or may even recover normal ventricular function, whereas others are symptomatic and may develop arrhythmias and progressive heart failure.[1] Unfortunately, our ability to risk-stratify and characterize disease mechanisms in these patients remains limited, and improved biomarkers are needed.[1,9,10]

Clinical Perspective on p 733

HCM and DCM are characterized by complex pathophysiological processes including impaired myocardial energetics,

Received April 3, 2012; accepted September 14, 2012.

From the University of Oxford Centre for Clinical Magnetic Resonance Research (OCMR), Department of Cardiovascular Medicine, John Radcliffe Hospital, Oxford, UK (S.D., J.J.S., S.K.P., V.M.F., C.J.H., R.B., M.M., T.D.K., M.D.R., H.W., S.N.); and Department of Physiology, Anatomy and Genetics, University of Oxford, Oxford, UK (C.J.H., L.C.).

*Drs Dass and Suttie contributed equally to this work.

Correspondence to Stefan Neubauer, MD, OCMR, Level 0, John Radcliffe Hospital, Headley Way, Headington, Oxford OX3 9DU, United Kingdom. E-mail stefan.neubauer@cardiov.ox.ac.uk

Circ Cardiovasc Imaging **is available at http://circimaging.ahajournals.org** **DOI: 10.1161/CIRCIMAGING.112.976738**

edema, myocardial fibrosis, and structural remodeling.[1] Cardiovascular magnetic resonance (CMR) imaging can provide insight into these processes with a number of myocardial tissue characterization techniques.

Myocardial energetics, as assessed by the phosphocreatine/adenosine triphosphate (PCr/ATP) ratio, using ^{31}P magnetic resonance spectroscopy, have been shown to be a more powerful independent predictor of mortality in DCM than New York Heart Association class or left ventricular ejection fraction (LVEF).[11,12] In HCM, PCr/ATP is reduced irrespective of the degree of hypertrophy or symptomatology.[12]

Focal myocardial fibrosis, as assessed by CMR late gadolinium enhancement (LGE) imaging, has recently been identified as a predictor of cardiac death in HCM and DCM and may be an important biomarker for risk stratification and therapeutic monitoring.[7,13–17] However, the quantification of fibrosis achieved by LGE has several limitations.[18,19] LGE is unable to detect diffuse fibrosis, and it relies on a comparison between unaffected normal myocardium and regions of focal myocardial damage. Furthermore, qualitative assessment of LGE is operator-dependent and can be difficult to compare reliably between scans or individuals. There are additional methodological variations from the use of semiquantitative analysis techniques, some centers using visual scoring, others an arbitrary threshold above remote myocardium.[20]

More recently, postcontrast T1 mapping has been used to quantify changes in extracellular volume in DCM[21] and HCM.[19] However, both LGE and postcontrast T1 mapping are confined to characterizing extracellular myocardial disease. Furthermore, postcontrast T1 mapping techniques require the administration of exogenous contrast agents. Although generally well tolerated, this is costly and can be problematic in the context of renal impairment, allergies, and multiple dosing. These limitations of LGE and postcontrast T1 mapping may be potentially overcome using noncontrast T1 quantification.

We hypothesized that further characterization of the myocardium in HCM and DCM can be accomplished by noncontrast T1 mapping, which measures a composite signal from both the intra- and extracellular compartments.[22] We, therefore, applied a recently validated, highly accurate, novel short breath-hold absolute T1 mapping technique, Shortened Modified Look-Locker Inversion recovery in patients with DCM and HCM.[13] We compared absolute noncontrast myocardial T1 values in HCM and DCM with established methods of LGE, circumferential strain rates, PCr/ATP ratio, and wall thickness obtained from cine imaging. Our results indicate that noncontrast T1 mapping has the potential to contribute to tissue characterization in these cardiomyopathies.

Methods

Ethics and Study Population

The study was approved by our institutional ethics committee, and informed written consent was obtained from all subjects.

Twenty-eight patients with HCM were recruited from the University of Oxford Inherited Cardiomyopathy clinic. The diagnosis of HCM was based on a genetic determination of a pathogenic mutation (14 MYBPC3 mutations; 6 MYH7 mutations), or in the absence of an identified mutation (8 subjects), HCM was defined as the presence of left ventricular hypertrophy not originating from other causes (≥15 or ≥12 mm in documented familial disease). All patients had a full Bruce protocol exercise tolerance test, and patients were excluded if there was evidence of epicardial coronary artery disease based on this test.

Eighteen DCM patients were identified from the Heart Failure clinics at the John Radcliffe Hospital, Oxford. They were included if they had echocardiographic left ventricular ejection fraction <45% and coronary angiography excluding flow limiting coronary artery disease. All recruits were Class II-III New York Heart Association and stable on optimum tolerated heart failure treatment for at least 6 months.

Normal controls (12 subjects) were nonsmokers, had no history of cardiac disease, hypertension, family history of cardiomyopathy or sudden death, and had a normal 12-lead ECG.

Enrolled subjects had no contraindications for MR scanning.

CMR Protocol

All CMR examinations were performed on a Siemens 3T Trio MR system (Siemens Healthcare Erlangen, Germany).

Cardiac Function and Indices

Cardiac volumes were calculated based on a series of single breath-hold balanced steady-state free precession cine images including horizontal and vertical long axis and multiple short-axis stack. Each slice was 8 mm thick with a 3 mm gap and was prospectively gated with echo time 1.5 ms, repetition time 3 ms, flip angle 50°.

Noncontrast T1 Mapping

Shortened Modified Look-Locker Inversion recovery T1 maps were generated from at least 3 short-axis images with variable inversion preparation time as described previously.[23] Typical acquisition parameters were: echo time (TE)/repetition time (TR) =1.07/2.14 ms, flip angle=35º, field of view=340×255 mm, matrix size=192×144, 107 phase-encoding steps, interpolated pixel size=0.9×0.9, GRAPPA=2, 24 reference lines, cardiac delay time TD=500 ms, 206 ms acquisition time for single image, phase partial Fourier 6/8. If necessary, shimming and center frequency adjustments were performed to generate images free from off-resonance artifacts.

Late Gadolinium Enhancement

A bolus of 0.1 mmol/kg of body weight of a gadolinium-based contrast agent (Gadodiamide, Omniscan; GE Healthcare, Amersham, UK) followed by a 10-mL saline flush was administered through an intravenous cannula inserted into the antecubital fossa. Electrocardiographically gated images were acquired after a 5-minute delay in long- and short-axis planes using a breath-hold T1 weighted segmented inversion recovery turbo-fast low-angle shot sequence.[24] Noncontrast T1 maps and late gadolinium imaging were acquired on at least 3 matching slices (basal, midventricular, apical).

Myocardial Strain Imaging

Strain imaging using left ventricular (LV) tagging was used to determine global midventricular systolic circumferential strain, as described previously.[25] A gradient echo-based high-resolution tagging pulse sequence was performed at the midventricular level of the LV. This slice exactly matched the midventricular slice used for noncontrast T1 and LGE imaging. All data were acquired during breath-hold and ECG-triggering to capture 90% of the R-R interval. Sequence parameters were: field of view 360 mm, slice thickness 6 mm, TR 25 ms, TE 7.4 ms, flip angle 10°, and heart phase interval <40 ms, giving 15–30 phases per cardiac cycle, depending on the heart rate.

^{31}P MR Spectroscopy

^{31}P magnetic resonance spectroscopy was acquired with a 3-dimensional acquisition-weighted chemical shift imaging technique[26] with 10 averages at the centre of K-space and ultrashort TE[27] to minimize T2 effects and first-order phase artifacts. Acquisition time was 8 minutes, and an optimized radiofrequency pulse[28] centred between γ and α-ATP resonance frequencies was used to ensure uniform excitation of all spectral peaks. Five Nuclear Overhauser Effect pulses (2.5 ms, 222.2 V separated by 80.5 ms) were used to increase signal to noise. Acquisition matrix was 16×8×8 and field of view was 240×240×200 mm. Three 25-mm saturation bands were used, 2 placed over chest wall muscle and 1 placed over liver. The chemical shift imaging grid was placed with a central voxel in the midventricular septum and rotated to maximize coverage of the septal myocardium. This anatomically matched the midventricular slice used for T1 mapping and LGE.

Image Analysis

All slices were divided into 6 segments using the anterior right ventricular–LV insertion point as reference.

Evaluation of LV Function and Wall Thickness

Using Argus and Syngo 2002B (Siemens Healthcare, Erlangen, Germany), LV short-axis epicardial and endocardial borders were manually contoured at end-diastole and end-systole for determining end-diastolic volume (EDV), end-systolic volumes (ESV), and stroke volume (SV). Myocardial mass was also calculated by subtracting the endocardial volume from the epicardial volume. LV mass was calculated based on prior knowledge of myocardial specific density (1.05 g/cm^3) and indexed to body surface area. End-diastolic wall thickness was determined for each segment using an in-house software MC-ROI (programmed by S.K.P. in Interactive Data Language v.6.1; www.ittvis.com).

Evaluation of Myocardial T1 Values

Short-axis T1 maps were manually contoured using MC-ROI software (Interactive Data Language v.6.1; www.ittvis.com) to outline the endo- and epicardium. Average T1 values per case and per segment were calculated. Care was taken to avoid LV cavity blood pool and potential partial volume effects at the endo- and epicardial borders.

Quality Assessment of T1 Maps

As T1 maps are derived from nonlinear estimation based on a sequential series of steady-state free precession images acquired after an inversion pulse,[23] factors such as off-resonance artifacts, breathing motion, and poor T1 model fit could lead to falsely high or low T1 values. The presence of off-resonance artifacts and diaphragmatic movement was assessed by examination of the raw T1 weighted steady-state free precession images. To assess for how well T1 model fitting was achieved for each T1 map, parametric maps of the goodness of fit (R^2 maps) were used. R^2 maps provide an additional means to identify areas with potentially compromised T1 accuracy. These tools allow critical assessment of the quality of T1 maps generated to increase the reliability of T1 mapping compared with some of the standard CMR modalities. Moreover, 18±7 segments per case were analyzable. A second blinded operator analyzed 8 randomly selected cases. The same analysis technique was used and results were compared using Bland–Altman method.

Evaluation of LGE

LGE images were quantified in MC-ROI. Hyperenhanced pixels were defined as those with signal intensities >2 SD above the mean signal intensity in remote normal myocardium in the same slice. The presence or absence of fibrosis was a dichotomy based on visual scoring from a blinded experienced operator (C.H.). The extent of fibrosis was expressed as the affected LGE volume fraction of each segment.

LGE analysis was performed independent from the T1 analysis by a blinded operator.

Evaluation of Myocardial Strain

Tagged images were analyzed by an experienced operator (J.J.S.), blinded to the T1 and LGE analysis, using Cardiac Image Modeller software (CimTag2D v7 Auckland Medical Research, Auckland, New Zealand). Semiautomated analysis was performed by aligning a grid to the myocardial tagging planes in end-diastole. End-systole was determined visually, and tags adjusted at each frame through the cardiac cycle to derive peak systolic circumferential strain for the midventricular slice, which was expressed as a percentage change from end-diastole. Normal strain has previously been described as −19±2[25]; impaired myocardial contractility is shown by a more positive value.

Evaluation of ^{31}P MR Spectroscopy

Spectra were direct current-corrected and baseline-corrected based on the last half of acquired data points. Spectral peaks were imported into jMRUI (Java Magnetic Resonance User Interface)[29] and fitted using the Advanced Method of Accurate, Robust, and Efficient Spectroscopic fitting algorithm[30] making use of prior knowledge relating to the relative peak frequencies, amplitudes, phases, and j-coupling patterns.

Spectral peak areas were corrected for the effects of nuclear overhauser effect using correction factors determined by prior experiment[28]: nuclear overhauser effect correction factors used PCr 0.80, β-ATP 0.88, α-ATP 0.88, γ-ATP 0.79, 2,3-diphosphoglycerate 0.70. Correction for radiofrequency saturation was calculated for each subject using the TR and experimentally determined excitation flip angle at the chosen voxel and T1 values from literature[31]: PCr 3.8 s, γ-ATP 2.4 s, α-ATP 2.5 s, β-ATP 2.7 s, 2,3-diphosphoglycerate 1.39 s, and phosphodiesterase 1.1 s. The resulting peak areas of the 3 ATP signals were averaged and corrected for blood contamination by subtracting 11% of the 2,3-diphosphoglycerate peak area.[11]

Statistical Analysis

All data are expressed as mean±SD and checked for normality using Kolmogorov–Smirnov test. Comparisons between the 3 groups were performed with analysis of variance with post hoc Bonferroni corrections for between-group comparisons. The χ^2 test or Fisher exact test was used to compare discrete data as appropriate. Bivariate correlations were performed using Pearson's method. Interobserver reproducibility of T1 mapping measurements was assessed by using the Bland–Altman method as well as intra-class coefficient analysis. Statistical tests were 2-tailed, and a P value of <0.05 was considered to indicate a statistically significant difference. All statistical analysis was performed with commercially available software packages (IBM SPSS Statistics, version 19.0, and MedCalc, version 12).

Results

Study Population

Patient characteristics are summarized in Table 1. There were no differences in age or sex between normal and HCM or DCM, although the DCM group was older than the HCM group (age 61±10 versus 48±13 years), which reflects the typical presentation of these diseases. As expected, the HCM group had significantly higher mass indices as well as ejection fractions, and reduced end-diastolic and end-systolic volumes. The DCM cohort had significantly larger end-diastolic and end-systolic volumes and substantially lower ejection fraction.

The hemoglobin in both groups was normal (HCM: 14.1±1.1 g/dL, range 12.1–15.9 g/dL; DCM: 13.7±1.2 g/dL, range 11.1–15.4 g/dL).

Both HCM and DCM cohorts were considered low risk for sudden cardiac death. In the DCM population, there were no individuals with syncope or ventricular arrhythmia. Table 2 describes the HCM cohort risk stratification.

T1 Relaxation Times in HCM, DCM, and Normal Controls

Mean T1 relaxation time per subject was significantly elevated in both HCM and DCM (HCM 1209±28 ms, DCM 1225±42 ms, normal 1178±13 ms, P<0.05; Figure 1).

Relationship Between T1 Values and LGE

Here 78% of HCM patients and 66% of DCM patients had at least 1 segment visually scored as having LGE. In HCM and DCM, there was a significant but modest correlation between T1 values per segment and fraction of segments with LGE >2 SD of normal remote myocardium (r=0.35, P<0.0001).

In HCM and DCM, T1 values were significantly higher in segments with LGE (HCM 1228±41 ms, DCM 1254±73 ms) than in those without (HCM 1192±79 ms, DCM 1217±52 ms,

Table 1. Baseline Characteristics of Normal Controls, HCM, and DCM Patients

	Normal (n=12)	HCM (n=28)	DCM (n=18)	*P*
Age, y	52±11	48±13	61±10*	<0.01
Male, % (n)	58 (7)	64 (18)	44 (8)	0.1
Rest pulse, bpm	58±11	58±9	63±13	0.3
Systolic BP, mm Hg	121±8	122±19	117±21	0.7
Diastolic BP, mm Hg	75±7	73±13	71±14	0.6
Smokers, % (n)	0 (0)	0 (0)	11 (2)	
Diabetes, % (n)	0 (0)	0 (0)	11 (2)	
Hypertension, % (n)	0 (0)	4 (1)	11 (2)	
Atrial fibrillation, % (n)	0 (0)	0 (0)	11 (2)	
Body surface area, m^2	1.9±0.2	2.0±0.3	1.9±0.3	0.9
β-blockers % (n)	0 (0)	54 (15)	83 (15)	
ARB/ACE inhibitor, % (n)	0 (0)	7 (2)	83 (15)	
LVEF, %	64±5	74±5‡	37±17*†	<0.001
LV EDV index, mL/m^2	80±14	62±21‡	91±36*†	<0.01
LV ESV index, mL/m^2	26±7	17±6‡	57±29*†	<0.001
LV mass index, g/m^2	59±14	85±33‡	73±19†	0.02
NYHA functional class		1.2±0.4	2.1±0.7	

Values are mean±SD.

LVEF indicates left ventricular ejection fraction; BP, blood pressure; LV, left ventricular; EDV, end-diastolic volume; ESV, end-systolic volume; ARB/ACE, angiotensin receptor blocker/angiotensin converting enzyme inhibitor; and NYHA, New York Heart Association.

*P<0.05 HCM vs DCM; †P<0.05 DCM vs normal; ‡P<0.05 HCM vs normal.

P<0.01). However, even in segments not demonstrating LGE, T1 values were significantly higher than normal (P<0.01) (Figure 2). Figure 3 shows examples of T1 maps and LGE images for matched slices.

Relationship Between T1 Values and Wall Thickness

The mean T1 values of all tertiles of wall thickness were significantly increased above normal T1 in both HCM and DCM (Figure 4). In addition, in HCM, there was a positive relationship of wall thickness and T1 values, with T1 values highest in the most hypertrophied segments. In DCM, there was a negative relationship with T1 values highest in the thinnest segments.

Relationship Between T1 Values and Circumferential Strain Rates

For the midventricular slice of all patients, there was a significant correlation between the mean noncontrast T1 relaxation time and the slice average circumferential strain (r=0.42, P<0.01). Interestingly, even in the slices without LGE, this correlation was maintained (r=0.56, P=0.04), suggesting that T1 values can reflect abnormal myocardial strain prior to the onset of LGE (Figure 5).

Relationship Between T1, LGE, and PCr/ATP

The mean T1 relaxation time and LGE volume fraction of the midventricular septum (ie, for the area over which the voxel was placed for the assessment for PCr/ATP) were measured. The mean septal T1 was prolonged in both HCM and DCM (HCM 1228±32 ms; DCM 1228±36 ms; normal 1190±20 ms, P<0.01). PCr/ATP ratios were 1.72±0.33 in HCM and 1.72±0.41 in DCM. These values are lower than values from normal volunteers published using the same acquisition protocol (2.14±0.37).[32] There was no significant association between LGE burden and PCr/ATP (r=0.22, P=0.65). However, there was a statistically significant negative correlation between T1 values and PCr/ATP (Figure 6). This was significant for the combined HCM and DCM group (r=–0.59, P<0.0001) and also individually for HCM (r=–0.49, P<0.01) and DCM (r=–0.61, P<0.01) groups. Figure 3 shows examples of representative ^{31}P MR spectra.

Table 2. Clinical Risk Stratification in HCM Cohort

	HCM (n=28)
No. of SCD risk factors (0/1/2/3 risk factors), % (n)	43, 47, 10, 0 (12, 13, 3, 0)
Family history of SCD, % (n)	50 (14)
Unexplained syncope, % (n)	4 (1)
NSVT on Holter monitor, % (n)	7 (2)
Abnormal exercise blood pressure response, % (n)	0 (0)
Maximum LV wall thickness ≥30 mm, % (n)	7 (2)
LV outflow tract gradient, % (n)	0 (0)
Left atrial size, mean±SD, cm	6.7±2.8

HCM indicates hypertrophic cardiomyopathy; LV, left ventricular; NSVT, nonsustained ventricular tachycardia; and SCD, sudden cardiac death.

Assessment of Reproducibility of T1 Mapping

There was excellent correlation between segment T1 estimates between both operators (r=0.92). A Bland–Altman plot showed average difference in estimates of –0.7%, and 95% CI of –4.7% and 3.3% (Figure 7). The intraclass correlation coefficient was 0.92 (95% CI 0.85%–0.95%).

Discussion

The principal finding of this study is that noncontrast T1 mapping achieves myocardial characterization in HCM and DCM beyond that achieved by established LGE techniques alone. We report for the first time that global myocardial noncontrast T1 values are significantly elevated in DCM and HCM compared with normal controls. As expected, myocardial segments with focal fibrosis identified by LGE showed higher T1 values; however, this correlation was only modest. Furthermore, T1 values were increased in segments

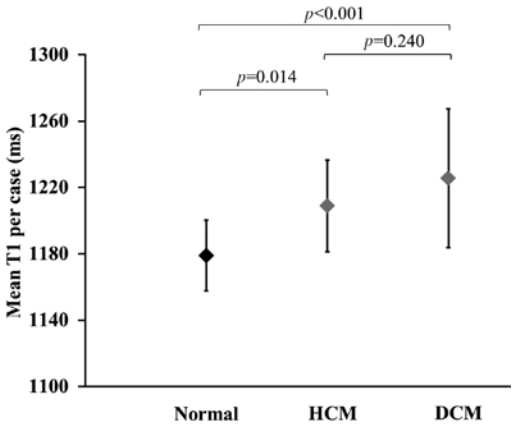

Figure 1. Myocardial T1 relaxation times in normal controls, hypertrophic cardiomyopathy (HCM), and dilated cardiomyopathy (DCM).

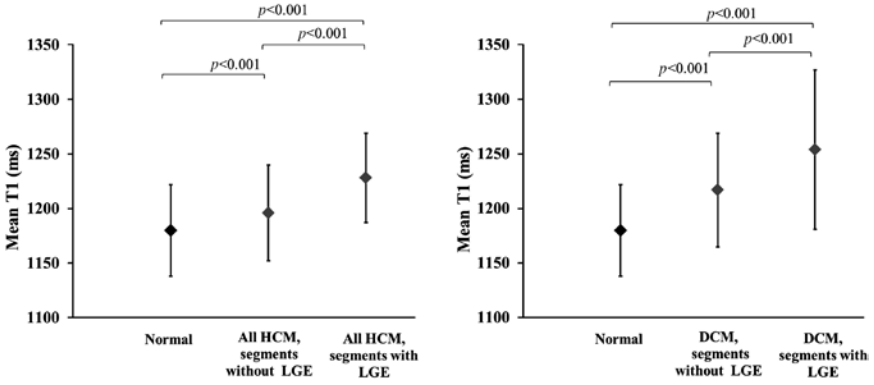

Figure 2. Myocardial T1 relaxation times in normal controls, segments with and without late gadolinium enhancement (LGE); **Left**, HCM; **Right**, DCM. Data represented are mean and SD.

without LGE in both HCM and DCM. This suggests that T1 mapping and LGE measure partly overlapping but distinct myocardial pathologies. As noncontrast T1 measures signal from the interstitium as well as the myocytes, both T1 values and LGE would be altered by expansion of the extracellular space, although noncontrast T1 values could be affected by additional changes such as intramyocellular water distribution, thereby potentially providing an additional level of insight.

Although T1 values only weakly correlated with LGE, T1 values correlated strongly with impaired myocardial energetics in both HCM and DCM. As we did not measure the intra- versus extracellular volume fraction in our study, we can only speculate on the mechanisms underlying this correlation. Experimental data have shown that myocardial scar contains negligible amounts of ATP,[33] and given that ATP is essential for PCr synthesis, the measured PCr and ATP signals are likely to arise from cardiomyocytes rather than from extracellular space. However, as extracellular fibrosis leads to myocardial stiffening,[34] periarteriolar fibrosis,[35] and diastolic dysfunction,[36] its presence may well affect the cardiomyocyte energetic state. Thus, it is possible that the more subtle changes detected by T1 values are a reflection of the extracellular matrix effects on the cardiomyocyte energetic state. It is also tempting to speculate that, as a second potential mechanism, energetically impaired myocardium in HCM and DCM is more vulnerable to membrane instability and ion pump dysfunction, resulting in intracellular fluid changes contributing to the T1 signal. Clearly, additional studies are needed, including larger patient numbers and assessment of intracellular versus extracellular volume fraction, in order to further elucidate these mechanisms and their relative contributions to energetic compromise. The finding of a statistically significant correlation of T1 values and circumferential strain, even in slices without LGE, also suggests that T1 mapping can detect functional changes in the myocardium prior to the development of fibrosis as measured by LGE.

Furthermore, there were significant associations between myocardial T1 values and ventricular wall thickness. In HCM, absolute T1 values were highest in the thickest myocardial segments; in contrast, myocardial T1 values in DCM were most

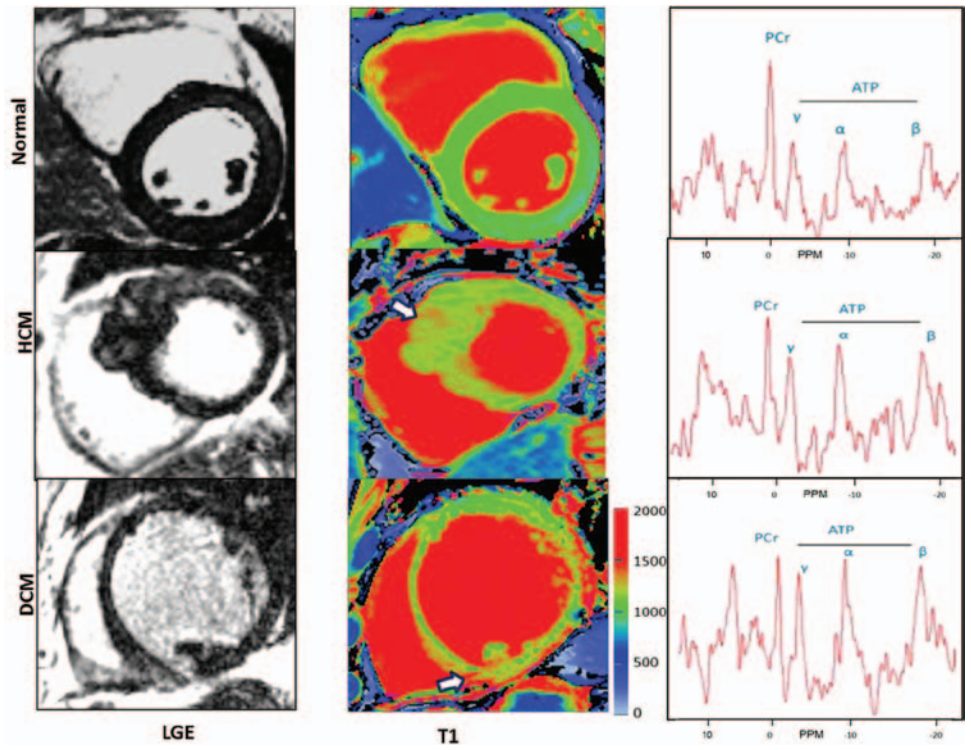

Figure 3. Late gadolinium enhancement (LGE) and T1 images in normal, hypertrophic cardiomyopathy (HCM), dilated cardiomyopathy (DCM). Arrows point to focal areas of LGE and high T1. Note: There is diffusely high T1 in the septum of HCM and inferior septum/inferior in the DCM. Representative spectra for each condition are shown; PCr indicates phosphocreatine; and ATP adenosine triphosphate.

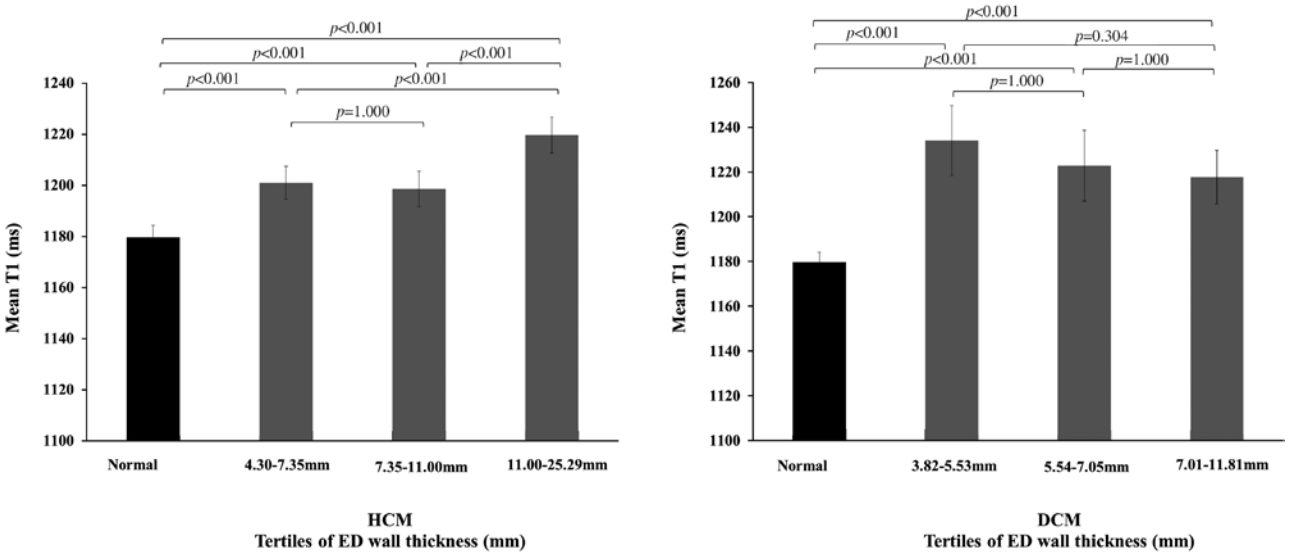

Figure 4. In hypertrophic cardiomyopathy (HCM) and dilated cardiomyopathy (DCM), mean T1 relaxation time plotted in tertiles of end-diastolic wall thickness; **error bars** are 95% CIs.

increased in the thinnest myocardial segments, with careful attention to avoid myocardial blood pool, suggesting that T1 values reflect the severity of the disease process in both HCM and DCM. Nonetheless, myocardial T1 values were elevated in HCM patients without left ventricular hypertrophy and in DCM patients without wall thinning, suggesting that T1 mapping may have additional application in the detection of early myocardial involvement in these cardiomyopathies.

Our findings confirm that, in this population, noncontrast T1 mapping is practical and reproducible in characterizing myocardial disease in patients with cardiomyopathy. All patients were able to tolerate the required breath-holds with comprehensive noncontrast T1 mapping of the LV acquired in <3 minutes.

Although our study yields interesting insights into the pathophysiology of HCM and DCM, the interindividual overlap of T1 values obtained with the current Shortened Modified Look-Locker Inversion recovery technique at 3T is too large to allow reliable initial diagnosis of individual patients. However, it is possible that with further sequence development and/or at higher field strength (eg, 7T), T1 differences may be sufficiently augmented to enable individual diagnosis by noncontrast T1 mapping. With this development, future work is also needed to explore the utility of noncontrast T1 mapping in characterizing genotype-positive HCM individuals who have not yet developed a hypertrophic phenotype. If this were achievable, T1 mapping may in the future have particular value for the assessment of hypertrophy-negative HCM patients, potentially adding diagnostic information when screening relatives of HCM patients where specific genes have not been identified. Furthermore, as the current Shortened Modified Look-Locker Inversion recovery method measures T1 with minimal intrasubject variation,[37] it may become a useful biomarker for monitoring treatment effects (eg, energy sparing therapy or antifibrotic therapy) in individual patients.

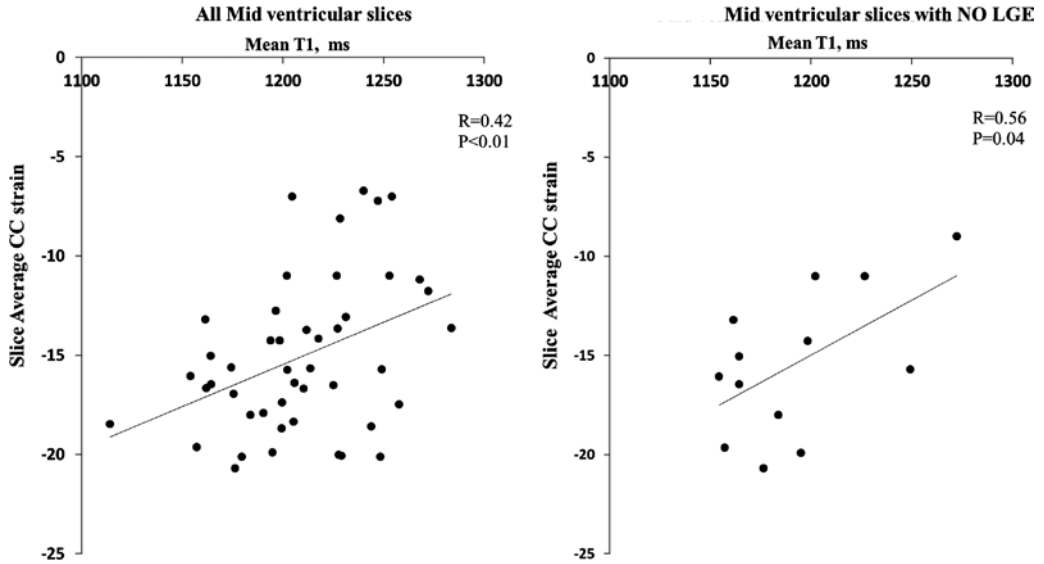

Figure 5. Left, Pearson's correlation between mean T1 and circumferential strain in midventricular slice of all subjects; **Right**, correlation in slices without late gadolinium enhancement (LGE).

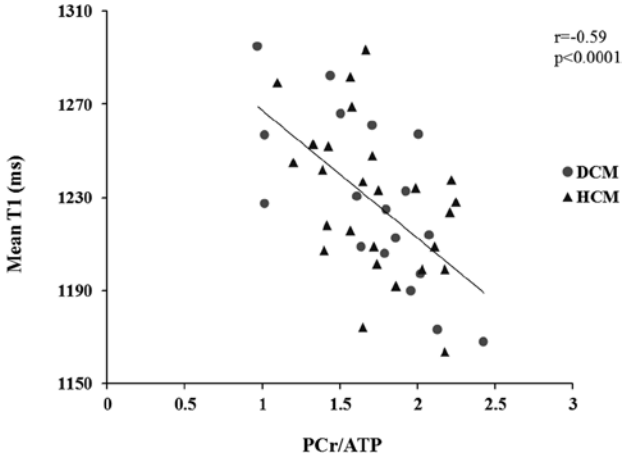

Figure 6. Scatterplot showing the correlation between phosphocreatine (PCr)/ATP and mean T1 in matching myocardium in hypertrophic cardiomyopathy (HCM) and dilated cardiomyopathy (DCM).

Limitations

Our study concentrated on the value of noncontrast T1 mapping for characterizing cardiomyopathies, and also on establishing a link between cardiac energetics and T1 relaxation. Additional measurement of postcontrast T1 provides information on the extracellular volume fraction, and such measurements could further assess the relative contribution of extracellular and intracellular water changes to the measured noncontrast T1 values. Thus, a limitation of this study is that postcontrast T1 mapping was not undertaken, and future studies should examine this. Another important intrinsic limitation of this study is the lack of histological correlation. Endomyocardial biopsies for research incur a significant risk that is difficult to justify without direct clinical benefit to the patient, and would be unethical in normal volunteers. Furthermore, biopsy validation is limited by sampling error in heterogeneous disease states.

This study has a relatively small sample size, and further larger-scale investigations are needed to build upon these results.

Conclusion

Noncontrast T1 mapping is practical in patients with cardiomyopathies and detects changes within the myocardium beyond the traditional measures of wall thickness and presence of LGE. With further longitudinal follow-up and validation against clinical end points, noncontrast myocardial T1 mapping may become a useful and practical biomarker in the early detection of cardiomyopathies, for monitoring therapeutic trials and for assessing prognosis.

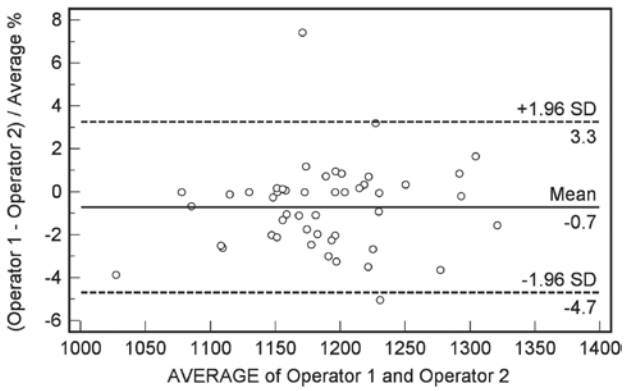

Figure 7. Bland–Altman plot demonstrating reproducibility of T1 analysis between 2 blinded operators.

Sources of Funding

The study was supported by fellowship grant FS/07/030 from the British Heart Foundation and by the Oxford Partnership Comprehensive Biomedical Research Centre with funding from the Department of Health's National Institute for Health Research Biomedical Research Centers funding plan. S.N. and H.W. acknowledge support from the Oxford BHF Center of Research Excellence. V.M.F. is funded by the Alberta Innovates Health Solutions (AIHS) Clinical Fellowship and the University of Oxford Clarendon Fund Scholarship.

Disclosures

Dr Piechnik has an ownership Interest in US patent pending 61/387,591: Systems and methods for shortened look locker inversion recovery (Sh-MOLLI) cardiac gated mapping of T1. Intellectual Property sold exclusively to Siemens Medical.

References

1. Watkins H, Ashrafian H, Redwood C. Inherited cardiomyopathies. *N Engl J Med*. 2011;364:1643–1656.
2. Towbin JA, Bowles NE. The failing heart. *Nature*. 2002;415:227–233.
3. Kelly DP, Strauss AW. Inherited cardiomyopathies. *N Engl J Med*. 1994;330:913–919.
4. Ho CY, Seidman CE. A contemporary approach to hypertrophic cardiomyopathy. *Circulation*. 2006;113:e858–e862.
5. Maron BJ, Gardin JM, Flack JM, Gidding SS, Kurosaki TT, Bild DE. Prevalence of hypertrophic cardiomyopathy in a general population of young adults. Echocardiographic analysis of 4111 subjects in the CARDIA Study. Coronary Artery Risk Development in (Young) Adults. *Circulation*. 1995;92:785–789.
6. McKenna WJ, Mogensen J, Elliott PM. Role of genotyping in risk factor assessment for sudden death in hypertrophic cardiomyopathy. *J Am Coll Cardiol*. 2002;39:2049–2051.
7. Assomull RG, Prasad SK, Lyne J, Smith G, Burman ED, Khan M, Sheppard MN, Poole-Wilson PA, Pennell DJ. Cardiovascular magnetic resonance, fibrosis, and prognosis in dilated cardiomyopathy. *J Am Coll Cardiol*. 2006;48:1977–1985.
8. Van Driest SL, Ellsworth EG, Ommen SR, Tajik AJ, Gersh BJ, Ackerman MJ. Prevalence and spectrum of thin filament mutations in an outpatient referral population with hypertrophic cardiomyopathy. *Circulation*. 2003;108:445–451.
9. Force T, Bonow RO, Houser SR, Solaro RJ, Hershberger RE, Adhikari B, Anderson ME, Boineau R, Byrne BJ, Cappola TP, Kalluri R, LeWinter MM, Maron MS, Molkentin JD, Ommen SR, Regnier M, Tang WH, Tian R, Konstam MA, Maron BJ, Seidman CE. Research priorities in hypertrophic cardiomyopathy: report of a Working Group of the National Heart, Lung, and Blood Institute. *Circulation*. 2010;122:1130–1133.
10. Priori SG, Aliot E, Blomstrom-Lundqvist C, Bossaert L, Breithardt G, Brugada P, Camm AJ, Cappato R, Cobbe SM, Di Mario C, Maron BJ, McKenna WJ, Pedersen AK, Ravens U, Schwartz PJ, Trusz-Gluza M, Vardas P, Wellens HJ, Zipes DP. Task Force on Sudden Cardiac Death of the European Society of Cardiology. *Eur Heart J*. 2001;22:1374–1450.
11. Neubauer S, Krahe T, Schindler R, Horn M, Hillenbrand H, Entzeroth C, Mader H, Kromer EP, Riegger GA, Lackner K. 31P magnetic resonance spectroscopy in dilated cardiomyopathy and coronary artery disease. Altered cardiac high-energy phosphate metabolism in heart failure. *Circulation*. 1992;86:1810–1818.
12. Crilley JG, Boehm EA, Blair E, Rajagopalan B, Blamire AM, Styles P, McKenna WJ, Ostman-Smith I, Clarke K, Watkins H. Hypertrophic cardiomyopathy due to sarcomeric gene mutations is characterized by impaired energy metabolism irrespective of the degree of hypertrophy. *J Am Coll Cardiol*. 2003;41:1776–1782.
13. O'Hanlon R, Grasso A, Roughton M, Moon JC, Clark S, Wage R, Webb J, Kulkarni M, Dawson D, Sulaibeekh L, Chandrasekaran B, Bucciarelli-Ducci C, Pasquale F, Cowie MR, McKenna WJ, Sheppard MN, Elliott PM, Pennell DJ, Prasad SK. Prognostic significance of myocardial fibrosis in hypertrophic cardiomyopathy. *J Am Coll Cardiol*. 2010;56:867–874.

14. Ho CYLB, Coelho-Filho O, Lakdawala NK, Cirino AL, Jarolim P, Kwong R, González A, Colan SD, Seidman JG, Díez J, Seidman CE. Myocardial fibrosis as an early manifestation of hypertrophic cardiomyopathy. *N Engl J Med*. 2010;363:552–563.
15. Bruder O, Wagner A, Jensen CJ, Schneider S, Ong P, Kispert EM, Nassenstein K, Schlosser T, Sabin GV, Sechtem U, Mahrholdt H. Myocardial scar visualized by cardiovascular magnetic resonance imaging predicts major adverse events in patients with hypertrophic cardiomyopathy. *J Am Coll Cardiol*. 2010;56:875–887.
16. Moon JC, McKenna WJ, McCrohon JA, Elliott PM, Smith GC, Pennell DJ. Toward clinical risk assessment in hypertrophic cardiomyopathy with gadolinium cardiovascular magnetic resonance. *J Am Coll Cardiol*. 2003;41:1561–1567.
17. Rubinshtein R, Glockner JF, Ommen SR, Araoz PA, Ackerman MJ, Sorajja P, Bos JM, Tajik AJ, Valeti US, Nishimura RA, Gersh BJ. Characteristics and clinical significance of late gadolinium enhancement by contrast-enhanced magnetic resonance imaging in patients with hypertrophic cardiomyopathy. *Circ Heart Fail*. 2010;3:51–58.
18. Mewton N, Liu CY, Croisille P, Bluemke D, Lima JA. Assessment of myocardial fibrosis with cardiovascular magnetic resonance. *J Am Coll Cardiol*. 2011;57:891–903.
19. Flett AS, Hayward MP, Ashworth MT, Hansen MS, Taylor AM, Elliott PM, McGregor C, Moon JC. Equilibrium contrast cardiovascular magnetic resonance for the measurement of diffuse myocardial fibrosis: preliminary validation in humans. *Circulation*. 2010;122:138–144.
20. Flett AS, Hasleton J, Cook C, Hausenloy D, Quarta G, Ariti C, Muthurangu V, Moon JC. Evaluation of techniques for the quantification of myocardial scar of differing etiology using cardiac magnetic resonance. *JACC Cardiovasc Imaging*. 2011;4:150–156.
21. Iles L, Pfluger H, Phrommintikul A, Cherayath J, Aksit P, Gupta SN, Kaye DM, Taylor AJ. Evaluation of diffuse myocardial fibrosis in heart failure with cardiac magnetic resonance contrast-enhanced T1 mapping. *J Am Coll Cardiol*. 2008;52:1574–1580.
22. White SK, Sado DM, Flett AS, Moon JC. Characterising the myocardial interstitial space: the clinical relevance of non-invasive imaging. *Heart*. 2012;98:773–779.
23. Piechnik SK, Ferreira VM, Dall'Armellina E, Cochlin LE, Greiser A, Neubauer S, Robson MD. Shortened Modified Look-Locker Inversion recovery (ShMOLLI) for clinical myocardial T1-mapping at 1.5 and 3 T within a 9 heartbeat breathhold. *J Cardiovasc Magn Reson*. 2010;12:69.
24. Selvanayagam JB, Jerosch-Herold M, Porto I, Sheridan D, Cheng AS, Petersen SE, Searle N, Channon KM, Banning AP, Neubauer S. Resting myocardial blood flow is impaired in hibernating myocardium: a magnetic resonance study of quantitative perfusion assessment. *Circulation*. 2005;112:3289–3296.
25. Lawton JS, Cupps BP, Knutsen AK, Ma N, Brady BD, Reynolds LM, Pasque MK. Magnetic resonance imaging detects significant sex differences in human myocardial strain. *Biomed Eng Online*. 2011;10:76.
26. Pohmann R, von Kienlin M. Accurate phosphorus metabolite images of the human heart by 3D acquisition-weighted CSI. *Magn Reson Med*. 2001;45:817–826.
27. Robson MD, Tyler DJ, Neubauer S. Ultrashort TE chemical shift imaging (UTE-CSI). *Magn Reson Med*. 2005;53:267–274.
28. Tyler DJ, Emmanuel Y, Cochlin LE, Hudsmith LE, Holloway CJ, Neubauer S, Clarke K, Robson MD. Reproducibility of 31P cardiac magnetic resonance spectroscopy at 3 T. *NMR Biomed*. 2009;22:405–413.
29. Naressi A, Couturier C, Castang I, de Beer R, Graveron-Demilly D. Java-based graphical user interface for MRUI, a software package for quantitation of in vivo/medical magnetic resonance spectroscopy signals. *Comput Biol Med*. 2001;31:269–286.
30. Naressi A, Couturier C, Devos JM, Janssen M, Mangeat C, de Beer R, Graveron-Demilly D. Java-based graphical user interface for the MRUI quantitation package. *MAGMA*. 2001;12:141–152.
31. Bottomley PA, Ouwerkerk R. Optimum flip-angles for exciting NMR with uncertain T1 values. *Magn Reson Med*. 1994;32:137–141.
32. Dass S, Cochlin L, Suttie J, Holloway C, Rodgers C, Tyler D, Karamitsos T, Clarke K, Watkins KSN. Exercise acutely exacerbates derangement of cardiac energy metabolism in hypertrophic cardiomyopathy, a 31 phosphorus magnetic resonance study at 3 telsa. *Circulation*. 2011;124:A15324.
33. Neubauer S, Horn M, Naumann A, Tian R, Hu K, Laser M, Friedrich J, Gaudron P, Schnackerz K, Ingwall JS. Impairment of energy metabolism in intact residual myocardium of rat hearts with chronic myocardial infarction. *J Clin Invest*. 1995;95:1092–1100.
34. Weber KT, Brilla CG. Pathological hypertrophy and cardiac interstitium. Fibrosis and renin-angiotensin-aldosterone system. *Circulation*. 1991;83:1849–1865.
35. Schwartzkopff B, Brehm M, Mundhenke M, Strauer BE. Repair of coronary arterioles after treatment with perindopril in hypertensive heart disease. *Hypertension*. 2000;36:220–225.
36. Brilla CG, Funck RC, Rupp H. Lisinopril-mediated regression of myocardial fibrosis in patients with hypertensive heart disease. *Circulation*. 2000;102:1388–1393.
37. Piechnik SFV, Lewandowski A, Ntusi N, Sado D, Maestrini V, White S, Lazdam M, Banerjee R, Hofman M, Moon J, Neubauer S, Leeson P, Robson M. Age and gender dependence of pre-contrast t1-relaxation times in normal human myocardium at 1.5t using shmolli. *J Cardiovasc Magn Reson*. 2012;14:P221.

CLINICAL PERSPECTIVE

Hypertrophic cardiomyopathy (HCM) is the commonest cause of sudden cardiac death in the young. Dilated cardiomyopathy (DCM) is the second most common cause of heart failure after coronary artery disease. As both HCM and DCM exhibit variable clinical outcomes, the ability to risk-stratify patients remains limited, and improved biomarkers are needed. Cardiac tissue characterization is possible with late gadolinium enhancement cardiac magnetic resonance, but this method only detects advanced tissue changes and requires magnetic resonance contrast agent. We demonstrate that further tissue characterization in HCM and DCM can be accomplished by noncontrast T1 mapping, which reflects composite signal from the interstitium and cardiomyocytes. We found that T1 relaxation is prolonged in DCM and HCM and T1 values correlate with LV circumferential strain, even in slices without focal fibrosis assessed by late gadolinium enhancement. Furthermore, T1 values (but not late gadolinium enhancement) show a strong inverse correlation with myocardial energetics, as measured by the phosphocreatine/ATP ratio, which may be because of changes in the extracellular matrix and increased intracellular water content because of membrane instability in energetically compromised cardiomyocytes. In addition, T1 is related to increased wall thickness in HCM and reduced wall thickness in DCM, suggesting that T1 also reflects disease severity. T1 mapping can detect abnormal myocardial tissue characteristics in HCM and DCM, beyond the traditional measures of wall thickness and late gadolinium enhancement. Future studies will have to validate T1 changes against clinical end points. Noncontrast T1 mapping has the potential to become a useful biomarker in the early detection and risk-stratification of cardiomyopathies.